ELSEVIER

Chemical Geology 175 (2001) 689–701

CHEMICAL GEOLOGY
INCLUDING
ISOTOPE GEOSCIENCE

www.elsevier.com/locate/chemgeo

An improved approach to calculating low-energy cosmic-ray neutron fluxes near the land/atmosphere interface

Fred M. Phillips [a,*], William D. Stone [b], June T. Fabryka-Martin [c]

[a] *Earth and Environmental Science Department, New Mexico Tech, Socorro, NM 87801, USA*
[b] *Mathematics Department, New Mexico Tech, Socorro, NM 87801, USA*
[c] *Los Alamos National Laboratory, Group E-ET, MS J514, Los Alamos, NM 87545, USA*

Received 5 October 1999; accepted 7 June 2000

Abstract

Low-energy cosmic-ray neutrons play an important role in the production of the cosmogenic nuclides ^{36}Cl and ^{41}Ca. Previous approaches to modeling the distribution of low-energy neutrons beneath the surface of the earth have derived the thermal neutrons directly from the high-energy neutron flux. We have improved on this model by deriving the thermal neutrons from the moderation of the epithermal neutron flux, and the epithermal neutrons from the fast neutron flux. Predictions from the improved model agree well with experimental measurements of thermal and epithermal neutron fluxes both above and below the land/atmosphere interface. Recalibration of the ^{36}Cl surface production parameters of Phillips et al. [Phillips, F.M., Zreda, M.G., Flinsch, M.R., Elmore, D., Sharma, P., 1996. A reevaluation of cosmogenic ^{36}Cl production rates in terrestrial rocks. Geophys. Res. Lett., 23, pp. 949–952), incorporating the new approach to simulating the low-energy neutron fluxes, yielded the following values: $P_{s,Ca}$ 66.8 atoms (g Ca)$^{-1}$ year^{-1}, $P_{s,K}$ 137 atoms (g K)$^{-1}$ year^{-1}, and $P_f(0)$ 626 neutrons (g air)$^{-1}$ year^{-1} (this updated calibration also includes mugenic ^{36}Cl production, based on independent work). Comparison of ages of three groups of samples from sites not included in the calibration data set with independently determined ages gave an average absolute error of 6.6% for all three data sets and coefficients of variation among the samples in the groups ranging from 5% to 14%.

Keywords: Cosmogenic elements; Exposure age; Cl-36; Neutron methods; Absolute age; Cosmochemistry

1. Introduction

Galactic cosmic radiation originates from outside the solar system and consists largely of high-energy protons and heavier atomic nuclei (Gaisser, 1990). Reactions of this primary cosmic-ray flux with nuclei of gas atoms in the upper atmosphere creates a cascade of secondary radiation that penetrates through the atmosphere down to the surface of the earth (Lal and Peters, 1967). Most of the nucleonic cosmic-ray flux that reaches the surface of the earth consists of neutrons. The higher-energy component of this secondary radiation is attenuated in exponential proportion to the cumulative mass traversed by the cosmic-

* Corresponding author. Tel.: +1-505-835-5540; fax: +1-505-835-6436.
E-mail address: phillips@nmt.edu (F.M. Phillips).

0009-2541/01/$ - see front matter
PII: S0009-2541(00)00329-6

ray beam, and is relatively independent of whether the radiation is passing through the atmosphere or the solid earth (Lal, 1991). In contrast, the low-energy neutrons behave in a diffusive fashion and their fluxes are strongly dependent on the composition of the medium through which they move (Bethe et al., 1940). This characteristic creates a rather complex distribution of low-energy neutron fluxes at the land/atmosphere interface.

The behavior of neutrons at the land/atmosphere interface assumed a new degree of importance with the advent of terrestrial, in situ, cosmogenic nuclide studies about 15 years ago (Cerling and Craig, 1994). Two of the measurable terrestrial cosmogenic nuclides, ^{36}Cl and ^{41}Ca, are produced by low-energy neutron absorption reactions. They are usually sampled at the surface of the earth in order to measure exposure ages or erosion rates. Application of these nuclides to geological problems therefore requires the ability to calculate low-energy neutron fluxes at the land/atmosphere interface.

Liu et al. (1994) have previously presented an analytical solution for the distribution of the thermal neutron flux at the interface. This formulation, however, suffered from some significant limitations. Liu et al. (1994) warned: "The limitations [of our approach] that are inherent in its basic assumptions should be emphasized. Probably the most critical of these is the neglect of intermediate energy interactions. Variations in the rate of neutron thermalization can potentially have a profound effect on the thermal neutron distribution. Hydrogen is the most effective neutron energy moderator, and ... water content can very strongly influence the thermal neutron distribution with depth. [Our formulation] ... will probably be significantly in error for moist soils, or circumstances where water or snow cover the surface for significant periods of time." In this paper, we address these limitations by deriving an improved approach to calculating the low-energy neutron fluxes that accounts for neutron energy moderation effects, provides epithermal as well as thermal neutron fluxes, and allows incorporation of the effect of water on the distribution of the thermal flux. We then update the ^{36}Cl production rate calibration previously presented by Phillips et al. (1996) by incorporating the new epithermal and thermal diffusion formulations. We also incorporate the effects of muon production of ^{36}Cl into the calibration, based on the work of Stone et al. (1998).

2. Cosmogenic neutron fluxes

Cosmic-ray neutrons are produced throughout the atmosphere and upper few meters of the earth's crust due to bombardment of nuclei by high-energy cosmic rays. Each high-energy collision typically produces three to eight neutrons, each neutron having an average energy of 1 MeV, ranging up to 10 MeV, or even higher (Yamashita et al., 1966). These neutrons lose kinetic energy through collisions with surrounding nuclei. Collisions with heavy nuclei transfer little energy and thus many collisions are required to reach the thermal regime, whereas collisions with light nuclei (especially hydrogen) effectively transfer energy to the target nucleus and thus rapidly moderate the cosmic-ray neutrons to low energies.

The high-energy cosmic-ray flux originates from outside the atmosphere and propagates downward, thus there is a net flux of both particles and energy in the downward direction. In contrast, by the time the cosmic-ray neutrons reach the epithermal energy regime ($0.5\ \text{eV} < E_n < 1\ \text{keV}$), particle paths have been thoroughly randomized and the average behavior of the neutron flux is diffusive. The propensity for absorption of the neutrons into the nuclei of atoms with which they collide generally increases as the neutron energy decreases. Ultimately, those neutrons that are not absorbed during the energy moderation process are slowed down to the thermal energy regime, i.e., they possess only the kinetic energy dictated by the temperature of the ambient environment. For earth-surface environments, we consider the thermal regime to lie between 0.5 and 0 eV, with a typical average energy of ~ 0.025 eV. These thermal neutrons are most readily absorbed — or "captured" — into the nuclei of certain atoms, predominantly Fe, Ti, Si, K, Gd, Cl, and B in most common types of rocks (Leavy, 1987). In this paper, we refer to neutrons in both the epithermal and thermal energy ranges as "low-energy neutrons."

The source for neutrons in each energy range is the moderation of neutrons of higher energy. The sink for neutrons in each energy range (except the thermal range) is twofold: moderation of neutron

energy out of the range and absorption. In the thermal range, since it is by definition the lowest energy possible in the particular environment, the only sink is absorption. The complexity of neutron behavior at the land/atmosphere interface is largely a result of the contrasting neutron absorption properties of the atmosphere and typical earth surface materials. In the epithermal energy range, it is largely the energy moderation properties that dominate the loss of neutrons from the range. On a mass basis, the ability of the atmosphere to moderate epithermal neutrons is about an order of magnitude better than that of most dry rocks. However, due to the very effective energy moderation properties of hydrogen, small amounts of water in rock or soil will greatly increase its bulk moderation properties. Saturated soil is about five times as effective as the atmosphere in moderating epithermal neutrons. As a result of these changes in material properties with water content, dry soil usually has much higher epithermal neutron fluxes than the atmosphere, but wet soil has lower epithermal fluxes.

Thermal neutron fluxes, on the other hand, are much less dependent on water content. The only sink for thermal neutrons is absorption, and thus, it is the contrast in bulk thermal neutron absorption properties that determines the distribution of thermal neutron fluxes at the interface. Nitrogen has a very large thermal neutron absorption cross-section, and as a result, the macroscopic (bulk) absorption of the atmosphere is about one order of magnitude larger than that of most types of rock. Thermal neutron fluxes are therefore typically high in rock or soil and low in the atmosphere.

3. Distribution of the epithermal neutron flux

Liu et al. (1994) obtained an equation describing the variation of the thermal neutron flux around the land/atmosphere interface by simultaneously solving thermal-neutron diffusion equations for the atmosphere and subsurface. They assumed that the thermal neutrons were derived directly from the high-energy or "fast" neutron flux. In this paper we take a similar approach, but we perform a two-stage derivation: first deriving epithermal neutrons from the fast neutron flux, and then thermal neutrons from the epithermal flux. This approach permits both the epithermal and thermal fluxes to be calculated, and allows the effects of energy-moderating elements, such as hydrogen, to be incorporated.

Analogously to Liu et al. (1994), we assume that the epithermal neutron flux is governed by two linked diffusion equations of the form:

$$D_{\mathrm{eth},i}\frac{\mathrm{d}^2\Phi_{\mathrm{eth},i}}{\mathrm{d}Z^2}=\frac{\Phi_{\mathrm{eth},i}}{\Lambda_{\mathrm{eth},i}}-R_{\mathrm{eth},i}P_{\mathrm{f}}(Z) \tag{1}$$

The two equations are for $i=\mathrm{a}$ and $i=\mathrm{ss}$, where a refers to the atmosphere and ss refers to the subsurface. The left-hand side of Eq. (1) represents the diffusive loss ("leakage") of epithermal neutrons per unit mass per unit time. The first term on the right-hand side is the rate of loss of epithermal neutrons by energy moderation and resonance absorption and the second term is the rate of production of epithermal neutrons by moderation of higher-energy cosmic-ray neutrons. This formulation is based on standard neutron diffusion theory employed in nuclear reactor engineering (e.g., Glasstone (1955), Eq. 3.18.1). Z is mass depth (g cm^{-2}), the cumulative mass traversed per unit area as a function of linear distance from the reference plane, which is the land surface (by convention, Z is positive for depth below, and negative for height above, this surface). $D_{\mathrm{eth},i}$ is the epithermal neutron diffusion coefficient (g cm^{-2}) for medium i, calculated according to:

$$D_{\mathrm{eth},i}=\left[3\Sigma_{\mathrm{sc},i}\left(1-2\left(3\bar{A}_i\right)^{-1}\right)\right]^{-1} \tag{2}$$

$\Sigma_{\mathrm{sc},i}$ is the macroscopic neutron scattering cross-section (cm^2 g^{-1}) in material i:

$$\Sigma_{\mathrm{sc},i}=\sum_k \sigma_{\mathrm{sc},k}N_{k,i} \tag{3}$$

$\bar{A}_i$ is the average atomic weight of material i, $\sigma_{\mathrm{sc},k}$ is the elemental neutron scattering cross-section of element k (cm^2 atom^{-1}; values for the elemental low-energy neutron transport properties are given in

Table 1
Elemental values for low-energy neutron transport parameters, from Fabryka-Martin (1988)

k	A_i (g mol^{-1})	ξ_i (unitless)	$\sigma_{sc,i}$ (10^{-24} cm^2 atom^{-1})	$\sigma_{th,i}$ (10^{-24} cm^2 atom^{-1})	$I_{a,i}$ (10^{-24} cm^2 atom^{-1})
O	16	0.12	3.76	0.0002	0.0004
H	1	1	20.5	0.33	0
C	12	0.158	4.74	0.0034	0.0016
Na	23	0.084	3.025	0.53	0.311
Mg	24.3	0.08	3.42	0.063	0.038
Al	27	0.072	1.41	0.23	0.17
Si	28.1	0.07	2.01	0.17	0.127
P	31	–	5	0.2	–
K	39.1	0.05	2.04	2.15	1
Ca	40.1	0.049	2.53	0.43	0.235
Ti	47.9	0.041	4.09	6.1	3.1
Mn	54.9	0.036	2.2	13.3	14
Fe	55.8	0.035	11.35	2.56	1.39
Cl	35.5	0.055	15.8	33.5	13.7
B	10.8	0.174	4.27	767	1722
Sm	150.4	0.013	38	9640	1400
Gd	157.3	0.013	172	41 560	390

Table 1), and $N_{k,i}$ is the concentration of element k in material i (atoms g^{-1}). $\bar{A}_i$ is given by:

$$\bar{A}_i = \frac{\sum_k A_k N_{k,i}}{\sum_k N_{k,i}} \quad (4)$$

where A_k is the atomic weight of element k (g mol^{-1}). A_a is equal to 14.5 g mol^{-1}. The quantity "2" in Eq. (2) also has units of g mol^{-1}. The term $1 - 2(3A_i)^{-1}$ accounts for anisotropic scattering of the epithermal neutrons.

$\Phi_{eth,i}$ is the epithermal neutron flux (n cm^{-2} s^{-1}). Note that this quantity is independent of the direction of individual neutrons (i.e., a scalar) and is therefore the equivalent of neutron concentration rather than a net directional transport in the usual sense of a flux. For this derivation, the datum is the land surface; positive is downward and negative upward. Following Glasstone (1955), Eq. 3.82.1, the effective epithermal neutron attenuation length (g cm^{-2}) is given by:

$$\Lambda_{eth,i} = \left[\bar{\xi}_i (I_{eff,i} + \Sigma_{sc,i}) \right]^{-1} = \Sigma_{eth,i}^{-1} \quad (5)$$

where $\bar{\xi}_i$ is the macroscopic (average) log decrement energy loss per neutron collision:

$$\bar{\xi}_i = \frac{\sum_k \xi_k \sigma_{sc,k} N_{k,i}}{\sum_k \sigma_{sc,k} N_{k,i}} \quad (6)$$

$I_{eff,i}$ is the effective resonance integral for absorption of epithermal neutrons by material i and is given by:

$$I_{eff,i} = \sum_k (I_a)_k N_{k,i} \quad (7)$$

where $(I_a)_k$ is the dilute resonance integral for epithermal neutron absorption by element k (note that the "a" in this term refers to "absorption" rather than "atmosphere"). $\Sigma_{eth,i}$ is the effective epithermal loss (by both absorption and energy moderation) cross-section (cm^2 g^{-1}).

P_f is the production rate (n g^{-1} year^{-1}) of epithermal neutrons from fast (i.e., energetic: $\sim$1 to 10 MeV) secondary cosmogenic neutrons. Following the standard model, we assume that the fast neutron flux follows an exponential distribution with cumula-

tive mass depth (see Liu et al., 1994; Lal, 1991; Gosse and Phillips, 2000):

$$P_f(Z) = P_f(0)\exp\left(-\frac{Z}{\Lambda_f}\right) \quad (8)$$

$P_f(0)$ is the production rate of epithermal neutrons from fast neutrons in the atmosphere at the land/atmosphere interface and Λ_f is the fast neutron attenuation length (g cm^{-2}), which has been empirically established to be in the range 140 to 170 g cm^{-2}, depending on latitude (Cerling and Craig, 1994). $R_{eth,i}$ (dimensionless) is the normalization factor for the neutron production rate and according to Dep et al. (1994) is given by:

$$R_{eth,i} = \left(\frac{A_i}{A_a}\right)^{1/2} \quad (9)$$

$R_{eth,a}$ is equal to unity.

The general solution of the coupled differential equations for atmosphere and for subsurface, of the form of Eq. (1), is given by:

$$\Phi_{eth,i}(Z) = C_{i,1}\exp\left(-Z\left(\frac{\Sigma_{eth,i}}{D_{eth,i}}\right)^{1/2}\right) + C_{i,2}\exp\left(Z\left(\frac{\Sigma_{eth,i}}{D_{eth,i}}\right)^{1/2}\right) + \frac{R_{eth,i}P_f(0)}{\Sigma_{eth,i} - D_{eth,i}\Lambda_f^{-2}}\exp\left(\frac{-Z}{\Lambda_f}\right) \quad (10)$$

The constants of integration in Eq. (10) can be solved using the boundary conditions listed below:

(i) $\Phi_{eth,ss}(\infty) = 0$ (the cosmic-ray flux is completely attenuated at an infinite depth)
(ii) $\Phi_{eth,ss}(0) = \Phi_{eth,a}(0)$ (continuity of concentration [commonly referred to as epithermal neutron flux] across the atmosphere/subsurface boundary)
(iii) $D_{eth,ss}(d\Phi_{eth,ss}(0)/dZ) = D_{eth,a}(d\Phi_{eth,a}(0)/dZ)$ (continuity of [true] epithermal neutron flux across the boundary)
(iv) $\Phi_{eth,a}(Z) = (P_f(0)/(\Sigma_{eth,a} - D_{eth,a}\Lambda_f^{-2}))\exp(-Z/\Lambda_f)$, $Z \ll 0$ (at large distances above the boundary the epithermal neutron flux is in spatial equilibrium with the atmospheric energetic neutron flux).

The solutions for the subsurface and atmospheric epithermal neutron fluxes are given by:

$$\Phi_{eth,i} = \Phi^*_{eth,i}\exp\left(-\frac{Z}{\Lambda_f}\right) + (F\Delta\Phi)^*_{eth,i}\exp\left(-\frac{|Z|}{L_{eth,i}}\right) \quad (11)$$

where $L_{eth,i}$ is the epithermal neutron diffusion length in medium i (g cm^{-2}), equal to $(D_{eth,i}/\Sigma_{eth,i})^{1/2}$, and

$$\Phi^*_{eth,i} = P_f(0)\frac{R_{eth,i}}{\Sigma_{eth,i} - D_{eth,i}/\Lambda_f^2} \quad (12)$$

$$(F\Delta\Phi)^*_{eth,i} = \frac{\frac{D_{eth,j}}{L_{eth,j}}\Delta\Phi^*_{eth,i} - \frac{D_{eth,ss}}{\Lambda_f}\Delta\Phi^{**}_{eth,a}}{\frac{D_{eth,a}}{L_{eth,a}} - \frac{D_{eth,ss}}{L_{eth,ss}}} \quad (13)$$

where

$$\Delta\Phi^*_{eth,i} = \Phi^*_{eth,j} - \Phi^*_{eth,i} \quad (14a)$$

and

$$\Delta\Phi^{**}_{eth,a} = \Phi^*_{eth,ss} - \frac{D_{eth,a}}{D_{eth,ss}}\Phi^*_{eth,a} \quad (14b)$$

i is the environment of interest (a or ss) and j is the other environment (i.e., if i = a, then j = ss). Physically, $\Phi^*_{eth,ss}$ represents the epithermal neutron flux (n cm^{-2} year^{-1}) that would be observed at the position of the land surface if the atmosphere had the same epithermal neutron transport properties as the subsurface and $\Delta\Phi^*_{eth}$ is the difference between the equilibrium epithermal neutron fluxes in a medium with the properties of the atmosphere and one with the properties of the subsurface. $(F\Delta\Phi)_{eth,i}$ represents the difference between the flux that would be observed at $Z = 0$ if only medium i were present and the flux actually observed in the presence of an interface.

4. Distribution of the thermal neutron flux

We assume that the thermal neutron flux is governed by a diffusion equation similar to Eq. (1), but, in contrast to Eq. (3) in Liu et al. (1994), we assume that the source term in the equation is the rate of moderation of the epithermal neutron flux, rather than the fast neutron flux:

$$D_{\mathrm{th},i}\frac{\mathrm{d}^2\Phi_{\mathrm{th},i}}{\mathrm{d}Z^2}=\frac{\Phi_{\mathrm{th},i}}{\Lambda_{\mathrm{th},i}} - R_{\mathrm{th},i}\frac{p(E_{\mathrm{th}})_{\mathrm{a}}}{\Lambda_{\mathrm{eth},i}}\left[\Phi^{*}_{\mathrm{eth},i}\exp\left(\frac{-Z}{\Lambda_{\mathrm{f}}}\right) + (F\Delta\Phi)^{*}_{\mathrm{eth},i}\exp\left(\frac{-|Z|}{L_{\mathrm{eth},i}}\right)\right] \quad (15)$$

where $p(E_{\mathrm{th}})_i$ is the resonance escape probability of medium i (i.e., the fraction of epithermal neutrons that survive moderation into the thermal energy regime without absorption):

$$p(E_{\mathrm{th}})_i=\exp\left(\frac{-I_{\mathrm{eff},i}}{\Sigma_{\mathrm{sc},i}}\right) \quad (16)$$

R_{th} is the ratio of epithermal neutrons produced in medium i that reach thermal energies to those produced in the atmosphere that reach thermal energies:

$$R_{\mathrm{th},i}=\frac{p(E_{\mathrm{th}})_i}{p(E_{\mathrm{th}})_{\mathrm{a}}} \quad (17)$$

$$\Lambda_{\mathrm{th},i}=\Sigma^{-1}_{\mathrm{th},i}=\left(\sum_k \sigma_{\mathrm{th},k}N_{k,i}\right)^{-1} \quad (18)$$

$$D_{\mathrm{th},i}=\left[3\Sigma_{\mathrm{sc},i}\left(1-2(3A_i)^{-1}\right)\right]^{-1} \quad (19)$$

Σ_{th} is the macroscopic thermal neutron absorption cross-section ($\mathrm{cm}^2\ \mathrm{g}^{-1}$) and $\sigma_{\mathrm{th},k}$ is the elemental thermal neutron absorption cross-section for element k (cm^2). (Note that σ_{th} is conventionally expressed in barns, where 1 barn $=10^{-24}$ cm^2). As with the epithermal neutron flux governing equation, Eq. (15) applies to both the atmosphere ($i=\mathrm{a}$) and the subsurface ($i=\mathrm{ss}$).

Eq. (15) can be solved simultaneously for the atmosphere and the subsurface, subject to the same four boundary conditions listed above for the epithermal neutron problem, except that "th" is substituted for "eth" and epithermal parameter values are used instead of the thermal values. The solutions for both materials can be expressed as:

$$\Phi_{\mathrm{th},i}=\Phi^{*}_{\mathrm{th},i}\exp\left(\frac{-Z}{\Lambda_{\mathrm{f}}}\right)+(\Im\Delta\Phi)^{*}_{\mathrm{eth},i}\exp\left(\frac{-|Z|}{L_{\mathrm{eth},i}}\right) + (\Im\Delta\Phi)^{*}_{\mathrm{th},i}\exp\left(\frac{-|Z|}{L_{\mathrm{th},i}}\right) \quad (20)$$

where $L_{\mathrm{th},i}$ is the thermal neutron diffusion length (g cm^{-2}) in medium i, equal to $(D_{\mathrm{th},i}/\Sigma_{\mathrm{th},i})^{1/2}$, and

$$\Phi^{*}_{\mathrm{th},i}=\frac{p(E_{\mathrm{th}})_{\mathrm{a}}R_{\mathrm{th},i}\Phi^{*}_{\mathrm{eth},i}}{\Lambda_{\mathrm{eth},i}\left(\Sigma_{\mathrm{th},i}-D_{\mathrm{th},i}/\Lambda^2_{\mathrm{f}}\right)} \quad (21)$$

$$(\Im\Delta\Phi)^{*}_{\mathrm{eth},i}=\frac{p(E_{\mathrm{th}})_{\mathrm{a}}R_{\mathrm{th},i}(F\Delta\Phi)^{*}_{\mathrm{eth},i}}{\Lambda_{\mathrm{eth},i}\left(\Sigma_{\mathrm{th},i}-D_{\mathrm{th},i}/L^2_{\mathrm{eth},i}\right)} \quad (22)$$

$$(\Im\Delta\Phi)^{*}_{\mathrm{th},i}=\Big[D_{\mathrm{th,a}}\left(\Phi^{*}_{\mathrm{th,a}}\Lambda^{-1}_{\mathrm{f}}-(\Im\Delta\Phi)^{*}_{\mathrm{eth,a}}L^{-1}_{\mathrm{eth,a}}\right) - D_{\mathrm{th,ss}}\left(\Phi^{*}_{\mathrm{th,ss}}\Lambda^{-1}_{\mathrm{th,ss}} + (\Im\Delta\Phi)^{*}_{\mathrm{eth,ss}}L^{-1}_{\mathrm{eth,ss}}\right) + \frac{D_{\mathrm{th},j}}{L_{\mathrm{th},j}}\left(\Delta\Phi^{*}_{\mathrm{th},i}+\Delta(\Im\Delta\Phi)^{*}_{\mathrm{eth},i}\right)\Big] \times\left[\frac{D_{\mathrm{th,ss}}}{L_{\mathrm{th,ss}}}+\frac{D_{\mathrm{th,a}}}{L_{\mathrm{th,a}}}\right]^{-1} \quad (23)$$

The terms $(\mathcal{T}\Delta\Phi)^{*}_{\mathrm{eth},i}$ and $(\mathcal{T}\Delta\Phi)^{*}_{\mathrm{th},i}$ quantify the deviations of the thermal neutron profile at the atmosphere/subsurface interface from one in the atmosphere only, due to the shape of the parent epithermal neutron profile and the subsequent diffusion of the thermalized neutrons across the interface, respectively. The other parameters in Eq. (23) are as follows:

$$\Delta\Phi^{*}_{\mathrm{th},j}=\Phi^{*}_{\mathrm{th},j}-\Phi^{*}_{\mathrm{th},i} \quad (24)$$

$$\Delta(\Im\Delta\Phi)^{*}_{\mathrm{eth},i}=(\Im\Delta\Phi)^{*}_{\mathrm{eth},j}-(\Im\Delta\Phi)^{*}_{\mathrm{eth},i} \quad (25)$$

Eqs. (11) and (20) can be combined to give the total subsurface production rate of any nuclide, m, that is

produced by absorption of low-energy cosmogenic neutrons:

$$P_{\mathrm{eth+th,ss},m} = \frac{f_{\mathrm{eth},m}}{\Lambda_{\mathrm{eth,ss}}}\Phi_{\mathrm{eth,ss}} + \frac{f_{\mathrm{th},m}}{\Lambda_{\mathrm{th,ss}}}\Phi_{\mathrm{th,ss}} \quad (26)$$

where:

$$f_{\mathrm{eth},m} = \frac{I_{\mathrm{a},k'}N_{k'}}{I_{\mathrm{eff,ss}}} \quad (27)$$

and

$$f_{\mathrm{th},m} = \frac{\sigma_{\mathrm{th},k'}N_{k'}}{\Sigma_{\mathrm{th}}} \quad (28)$$

where $f_{\mathrm{eth},m}$ and $f_{\mathrm{th},m}$ are, respectively, the fractions of the total epithermal and thermal neutrons that are absorbed by target nuclide k' (e.g., ^{35}Cl or ^{40}Ca) to produce nuclide m (e.g., ^{36}Cl or ^{41}Ca).

5. Comparison with experimental results

Unfortunately, there are few experimental data against which to compare our model simulations. In Liu et al. (1994), we have previously described one such experiment conducted at Los Alamos National Laboratory (2200 m elevation). Briefly, a concrete pad was constructed with horizontal tubes to serve as access for ^{3}He neutron counting tubes. The array of access tubes extended over a depth of 1 m. Counts were collected with both bare and Cd-shielded counters. From these data, the thermal and epithermal neutron fluxes can be calculated as a function of depth (calculation of the thermal flux from the difference between unshielded and Cd-shielded count rates was described in Liu et al. (1994), and the epithermal fluxes were calculated from the Cd-shielded count rates).

Fig. 1 shows the epithermal and thermal cosmic-ray neutron fluxes measured in the Los Alamos experiment, compared with the neutron fluxes calculated using Eqs. (11) and (20). Values for the material-dependent parameters in the equations were calculated using the concrete composition published in Liu et al. (1994). The water content of 13 vol.% from Liu et al. (1994) was used and a value of 626 n g^{-1} $year^{-1}$ specified for $P_f(0)$. This value comes

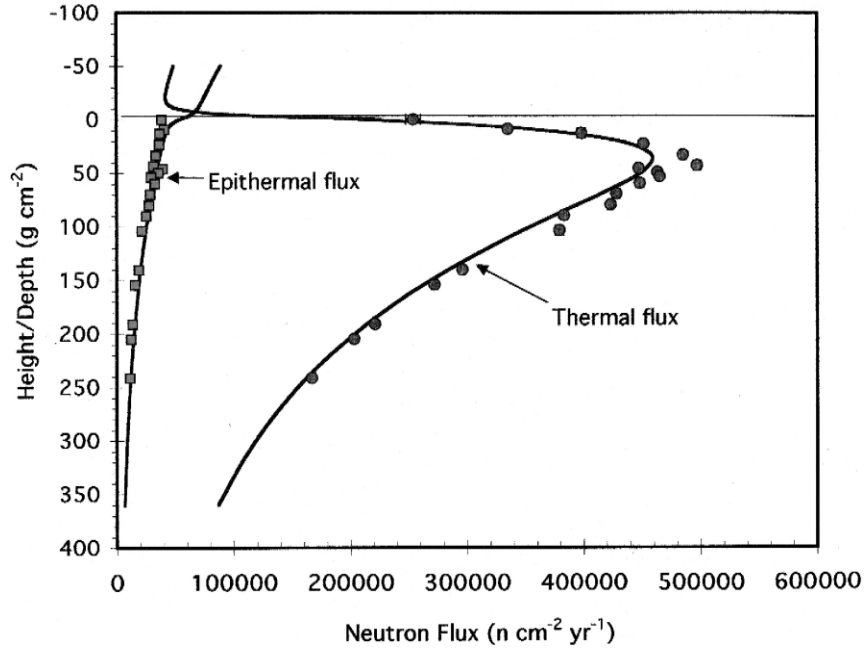

Fig. 1. Comparison of epithermal and thermal neutron fluxes measured in a concrete block at Los Alamos National Laboratory (Liu et al., 1994) with the distribution of these fluxes given by Eqs. (11) and (20). The epithermal flux measurements are given by squares and the thermal flux measurements by circles.

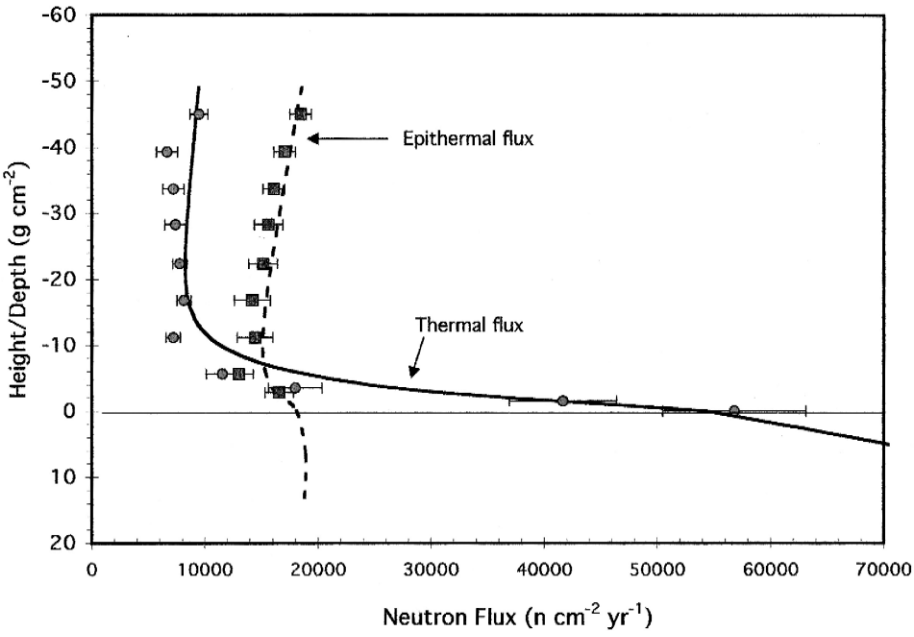

Fig. 2. Comparison of epithermal and thermal fluxes measured in air in South Carolina by Hendrick and Edge (1966) with the distribution of these fluxes given by Eqs. (11) and (20). The epithermal flux data are given by squares and the thermal flux data by circles.

directly from the recalibration described below. The agreement between the calculated and observed neutron fluxes is good.

Neutron fluxes in the air were not measured during the Los Alamos experiment. However, Hendrick and Edge (1966) conducted an experiment in South Carolina in which neutron counters were raised up a 450-m-high antenna tower. The differential neutron fluxes they reported were converted to fluxes within our specified epithermal and thermal energy ranges using an assumed average epithermal energy of 1.5 keV and an assumed average thermal energy of 0.6 eV. These average energy values are somewhat arbitrary, inasmuch as Hendrick and Edge (1966) did not actually determine the average energies sampled by their detectors, and described the epithermal and thermal average energies only as "about 1 keV" and "below $\sim$1 eV", respectively. Their measurements are compared with the fluxes predicted by Eqs. (11) and (20) in Fig. 2. Hendrick and Edge (1966) did not measure the composition of the soil beneath the tower, and we therefore used the composition of an average shale from Fabryka-Martin (1988). We employed their measured water content of 3.7%. Although the incompleteness of the experimental data makes comparison of the absolute fluxes rather uncertain, the shape of the observed and predicted fluxes agree well, as do the relative magnitudes of the thermal and epithermal fluxes.

6. Discussion

The comparisons with experimental data illustrated above indicate that Eqs. (11) and (20) adequately predict the epithermal and thermal cosmogenic neutron fluxes in, and above, earth materials. In particular, they are able to account for the effect of water on the moderation of epithermal neutrons. As shown in Fig. 3a, the epithermal flux is very strongly dependent on water content. Dry rock is a much poorer moderator of epithermal neutrons than is the atmosphere, hence, the epithermal flux in rock is much greater than in the atmosphere. However, the addition of even very small amounts of water greatly increases the moderating power of the rock (due solely to the increased concentration of H), dramatically decreasing the epithermal neutron flux.

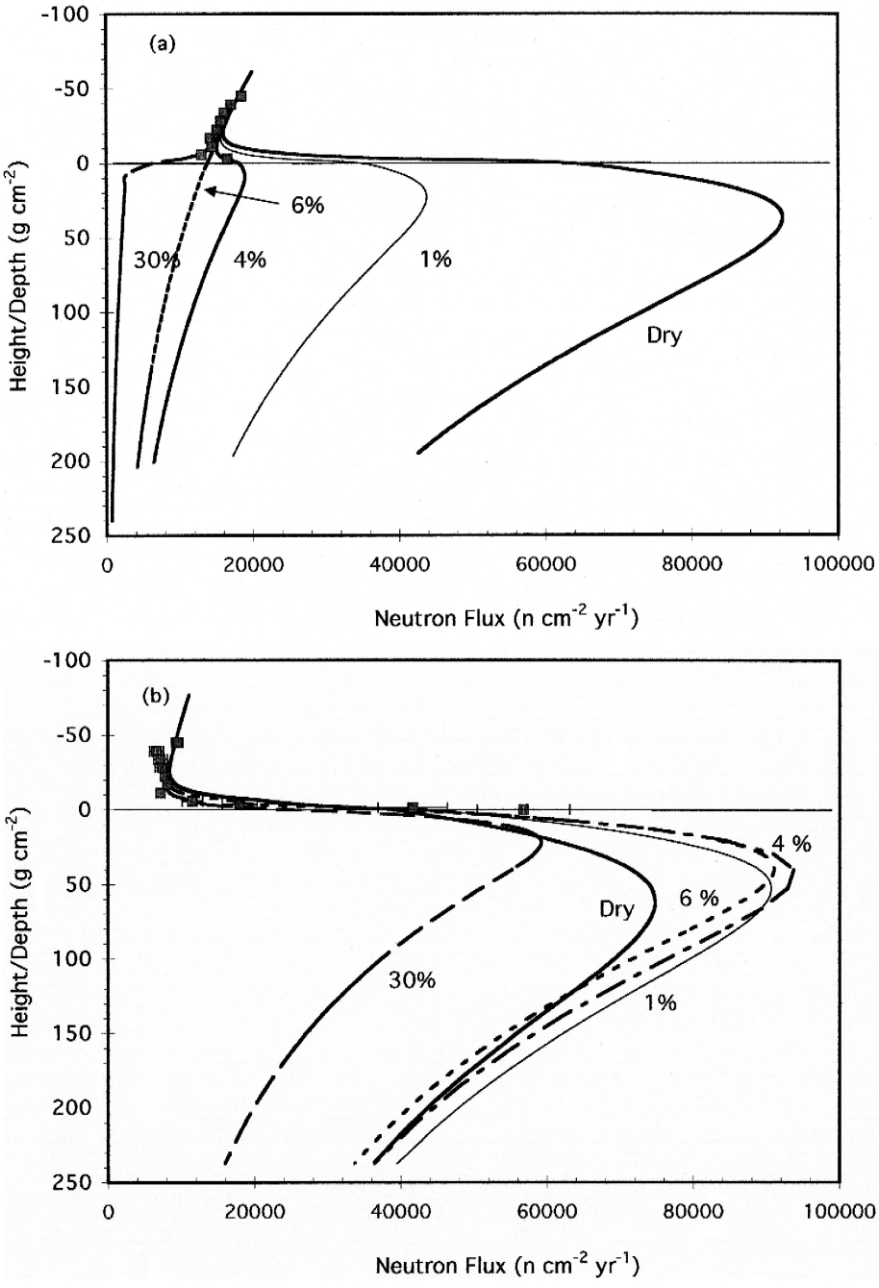

Fig. 3. (a) Epithermal neutron flux in average shale (Fabryka-Martin, 1988) as a function of water content, given in percent by each curve. The epithermal flux data of Hendrick and Edge (1966) are shown for comparison. The measured water content during the experiment of Hendrick and Edge (1966) was 3.7%. (b) Thermal neutron flux in average shale as a function of water content. The thermal flux data of Hendrick and Edge (1966) are shown for comparison.

In contrast, Fig. 3b shows that the thermal neutron flux is much less sensitive to water content. The thermal neutron flux initially increases as the water content of the rock increases above the completely

dry state because the reduced time spent by the neutrons in the epithermal energy range minimizes the potential for resonance absorption. However, as the water content increases above ~5%, the resultant increase in density and the thermal neutron absorption cross-section reduces the thermal neutron flux.

Fig. 4 illustrates the effect of changing water content on the production rate of ^{36}Cl. Two effects compete as the water content increases: the rate of thermalization of the epithermal neutrons increases, but so does the competition of the water itself for neutron absorption. At low water content (< 2%), there is a slight increase in the ^{36}Cl production rate as the water content increases. This is because the increased rate of thermalization decreases the rate at which epithermal neutrons diffuse into the atmosphere. However, above ~2% water content, the increased bulk density and increased competition for thermal neutrons by the water becomes the predominant effect and the ^{36}Cl production rate decreases. Accurate estimation of water content is not a critical problem for low-porosity rocks (such as typical crystalline rocks) or in dry climates, but becomes more important as the water content increases beyond 10%. Snow or ponded water on the rock surface will also have a significant effect, although it cannot be simulated with the simple two-medium solutions presented here.

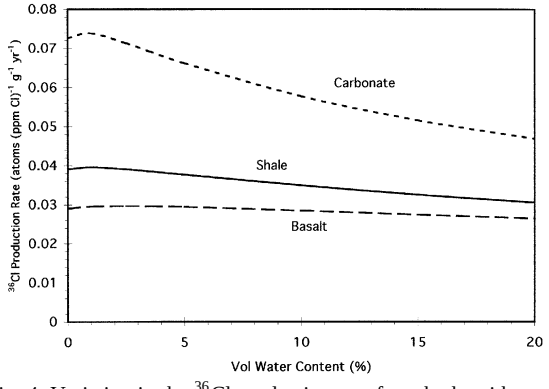

Fig. 4. Variation in the ^{36}Cl production rate from both epithermal and thermal neutron absorption by ^{35}Cl, as a function of water content, for average shale, basalt, and carbonate rocks (compositions from Fabryka-Martin, 1988). (Variation of production in granite is very similar to that in basalt.) Rocks were assumed to be at sea level and high latitude. Production rates are given per ppm Cl in order to normalize for varying Cl concentration.

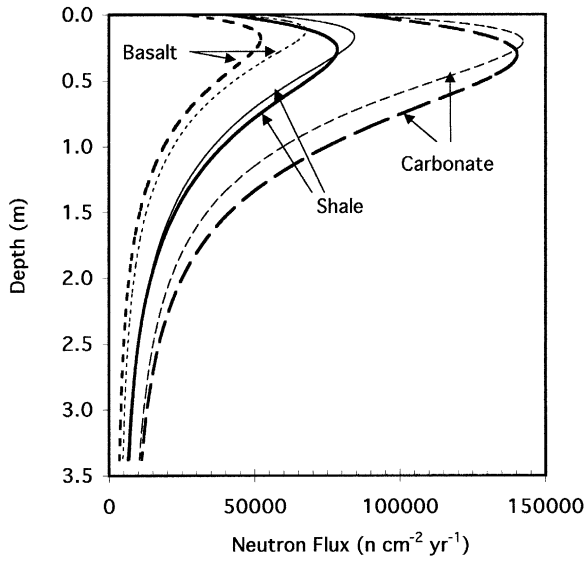

Fig. 5. Comparison of epithermal and thermal neutron fluxes in average carbonate, shale, and basalt (compositions from Fabryka-Martin, 1988). Epithermal fluxes are indicated by the thin lines and thermal fluxes by the thick lines. The rocks were assumed to be completely dry, and to be at high latitude and sea level.

The neutron flux distributions are significantly dependent on rock composition, as well as water content. Fig. 5 shows simulated thermal and epithermal neutron distributions in three common rock types: carbonate, shale, and basalt (the distribution in granite is very similar to that in basalt). For these calculations, all rock types are assumed to be dry. Both the magnitudes of the fluxes and the shapes of the profiles are sensitive to the elemental composition of the rock.

7. Updated ^{36}Cl production calibration

A major motivation for this work is to obtain more accurate surface exposure ages using cosmogenic nuclides produced by low-energy neutron absorption reactions, especially ^{36}Cl. Phillips et al. (1996) previously obtained production parameters for cosmogenic ^{36}Cl, based on a large data set of independently dated samples, using the thermal neu-

tron transport theory of Liu et al. (1994). The new parameterization of the low-energy neutron fluxes that is presented in this paper requires that these production parameters be recalibrated, since they are model-dependent. We therefore repeated the calibration of Phillips et al. (1996) using for the low-energy neutron production Eqs. (11) and (20) instead of the corresponding equations in Liu et al. (1994). The same data set as in Phillips et al. (1996) was employed (33 samples ranging in age from 2 to 55 ka) except that samples COM92-18, COM92-20, and MK-AT3B-28 were deleted from the data set. The first two were deleted because their analytical results deviated markedly from the results of multiple replicate samples from the same flows, and the last because of new doubts about the reliability of the K–Ar independent age. As previously, the production parameters were calculated by minimizing the reduced χ^2 parameter. However, a major difference from the procedure in Phillips et al. (1996) is these authors had explicitly excluded production of ^{36}Cl by muons (slow muon absorption by Ca, absorption of low-energy neutrons produced by slowing of fast muons, and photodisintegration reactions) whereas in this paper we account for muon production The formalism for including the muogenic production is given in Gosse and Phillips (2000) and is based on the results of Stone et al. (1998). It is important to emphasize that this "recalibration" does not include any new data, but is rather simply intended to make the model-dependent ^{36}Cl production parameters consistent with the new theoretical models presented above.

The recalibration yielded an increase of $\sim$7% in the fast neutron production parameter ($P_f(0)$), from 586 to 626 fast neutrons (g air)$^{-1}$ year^{-1} (all production parameters are normalized to high latitude and sea level). This is largely a result of the more accurate parameterization for low-energy neutron fluxes. The production constant for spallation of Ca ($P_{s,Ca}$) decreased by $\sim$9%, from 73.3 to 66.8 atoms ^{36}Cl (g Ca)$^{-1}$ year^{-1}. This is largely due to the explicit incorporation of ^{36}Cl production by slow muon absorption by Ca. The value of the production constant for spallation of K ($P_{s,K}$) was not changed from that of Phillips et al. (1996) because it was from a separate analysis (see Phillips et al., 1996) and this production constant is poorly constrained by this data set alone. The average deviation of the calculated ages from the control ages (the bias) decreased from 5.6% to 3.5%, but the value of the average absolute deviation, 12.6%, remained nearly the same as in the previous calibration. Phillips et al. (1996) also calculated production parameters that included a correction for secular variation of the production rates due to past variations in geomagnetic intensity. However, questions have recently been raised regarding the validity of the standard elevation/latitude scaling (Lal, 1991) by Dunai (2000), and until these are resolved, we will defer any similar analysis.

We checked both the accuracy and the precision of ages determined using the new theoretical basis and production parameters by calculating ^{36}Cl ages for three data sets that are completely independent of the calibration data set. The results are reported in

Table 2
Comparisons between independent ages and ages derived using the low-energy neutron formulations and production rates of this study

Site	Location	Number of samples	Material	Independent age (ka)	Average ^{36}Cl age (ka)	Standard deviation (ka)	Average error (%)	Average absolute error (%)
Egesen moraine	Switzerland	3	Mixed	11.6 ± 0.6	11.9	1.4	2.4	8.6
Lathrop Wells, all samples	Nevada, USA	16	Basalt	77 ± 4	63.5	9.0	−17.5	17.5
Lathrop Wells, 6 oldest samples	Nevada, USA	6	Basal	77 ± 4	72.1	3.7	−6.3	6.3
Recess Peak moraines	California, USA	9	Granodiorite	13.3 ± 0.3	12.9	0.7	−2.8	5.0
Mean (using six oldest LW samples)							*−2.2*	*6.6*

Table 2. The first sample set was three boulders from the Egesen moraines in the Swiss Alps, collected and analyzed by Ivy-Ochs et al. (1996). These moraines are firmly correlated with the Younger Dryas climate oscillation, dated by numerous methods to 12.1 to 11.0 ka. The lithology was mixed. We recalculated the boulder ages using the new theoretical basis and production parameters of this paper and obtained an average of 11.9 ± 1.4 ka. The second data set was 16 samples from the Lathrop Wells volcanic center in southern Nevada, USA. This small basaltic volcano has recently been dated to 77 ± 4 ka by $^{40}Ar/^{39}Ar$ (Heizler et al., 1999). We recalculated the ages of 11 samples reported by Zreda et al. (1993) and five more samples that we have analyzed subsequently. These yielded an average of 64 ± 9 ka. There is a significant possibility that some of these samples have temporarily been covered by sand, causing some scatter toward younger apparent ages. The mean and standard deviation of the six oldest samples is 72 ± 3.7 ka. The third data set consisted of nine samples from boulders on Recess Peak age moraines at the Treasure and Topsy-Turvey Lakes in the Bishop Creek drainage, and Third Lake in the Big Pine Creek drainage, in the Eastern Sierra Nevada, California. The sample lithology was granodiorite. The termination of the Recess Peak glaciation has been dated to 13.1 ± 0.085 calendar ka by radiocarbon measurements on basal sediments of lakes ponded behind the moraines (Clark and Gillespie, 1996). Given that this is a limiting minimum age, we have assumed a date of 13.3 ± 0.3 ka for the deposition of the terminal moraines. The mean and one standard deviation of the nine samples was 12.9 ± 0.7 ka (F.M. Phillips, unpublished data, 2000). In all three cases, and in spite of variable lithology, the ages obtained from these independent data sets appear to be acceptably accurate and reproducible. The coefficients of variation are 5% to 14% and the absolute average error 6.6%.

The comparisons given above indicate that the recalibrated production rates obtained from the theory given in this paper, together with the calibration data set of Phillips et al. (1996), gives satisfactory results when applied to independently constrained sample sets. However, there still remain significant and troublesome discrepancies with the ^{36}Cl production rates obtained by Stone et al. (1996) and Swanson (1996). Incomplete correction for elevation/latitude scaling (Dunai, 2000) may play a role in these discrepancies, but additional calibration samples and laboratory investigations are needed to resolve these problems.

8. Summary

The fluxes of low-energy cosmic-ray neutrons are strongly dependent on the elemental composition of earth materials, especially the water content. Previous formulations adequately simulated the depth-distribution of thermal neutrons, but did not adequately model the effects of energy moderation by water and other materials, on epithermal neutron fluxes. We have improved on the approach of Liu et al. (1994) and Phillips et al. (1996) by explicitly modeling the production and moderation of epithermal neutrons and the production of thermal neutrons from the epithermal flux. The predictions of the model show good agreement with experimental measurements of thermal and epithermal neutron fluxes.

The ^{36}Cl production parameters were recalibrated using the new low-energy neutron distribution equation, and also explicitly accounting for muogenic production. This resulted in a higher value for the fast neutron production parameter and a lower one for the calcium spallation parameter. A test of the recalculated production parameters against three independent data sets confirmed good accuracy and typical reproducibility of about 10%.

Acknowledgements

This research was partially supported by NSF grant EAR-9417810 and the U.S. Department of Energy contract 14-08-0001-22693 in cooperation with the the U.S. Geological Survey Yucca Mountain Project, the Institute of Geophysics and Planetary Physics (Los Alamos National Laboratory), and the Geosciences Research Program of the U.S. Department of Energy, Office of Basic Energy Science. We thank John Stone for a thorough and constructive review of the manuscript, and Mitchell A. Plummer and Brian Borchers for technical assistance.

References

Bethe, H.A., Korff, S.A., Placzek, G., 1940. On the interpretation of neutron measurements in cosmic radiation. Phys. Rev. 57, 573–587.

Cerling, T.E., Craig, H., 1994. Geomorphology and in-situ cosmogenic isotopes. Annu. Rev. Earth Planet. Sci. 22, 273–317.

Clark, D.H., Gillespie, A.R., 1996. Timing and significance of late-glacial and Holocene cirque glaciation in the Sierra Nevada, California. Quat. Int. 38/39, 21–38.

Dep, L., Elmore, D., Fabryka-Martin, J., Masarik, J., Reedy, R.C., 1994. Production rate systematics of in-situ produced cosmogenic nuclides in terrestrial rocks: Monte Carlo approach of investigating $^{35}Cl(n,\gamma)^{36}Cl$. Nucl. Instrum. Methods Phys. Res., Sect. B 92, 321–325.

Dunai, T.J., 2000. Scaling factors for production rates of in situ produced cosmogenic nuclides: a critical reevaluation. Earth Planet. Sci. Lett. 176, 157–169.

Fabryka-Martin, J.T., 1998. Production of radionuclides in the earth and their hydrogeologic significance, with emphasis on chlorine-36 and iodine-129. PhD Thesis, University of Arizona, Tucson, 400 pp.

Gaisser, T.K., 1990. Cosmic Rays and Particle Physics. Cambridge Univ. Press, Cambridge, 279 pp.

Glasstone, S., 1955. Principles of Nuclear Reactor Engineering. Van Nostrand-Reinhold, Princeton, NJ, pp. 132–168.

Gosse, J., Phillips, F.M., 2000. Terrestrial cosmogenic nuclides: theory and application. Quat. Sci. Rev. submitted for publication.

Heizler, M.T., Perry, F.V., Crowe, B.M., Peters, L., Appelt, R., 1999. The age of Lathrop Wells volcanic center: an $^{40}Ar/^{39}Ar$ dating investigation. J. Geophys. Res. 104, 767–804.

Hendrick, L.D., Edge, R.D., 1966. Cosmic-ray neutrons near the earth. Phys. Rev. 145, 1023–1025.

Ivy-Ochs, S. et al., 1996. The exposure age of an Egesen moraine at Julier Pass, Switzerland, measured with the cosmogenic radionuclides ^{10}Be, ^{26}Al and ^{36}Cl. Eclogae Geol. Helv. 89, 1049–1063.

Lal, D., 1991. Cosmic-ray labeling of erosion surfaces: in situ production rates and erosion models. Earth Planet. Sci. Lett. 104, 424–439.

Lal, D., Peters, B., 1967. Cosmic ray produced radioactivity on the earth. In: Sitte, K. (Ed.), Handbuch der Physik. Springer-Verlag, Berlin, pp. 551–612.

Leavy, B.D., 1987. Surface exposure dating of young volcanic rocks using the in situ buildup of cosmogenic isotopes. PhD dissertation, New Mexico Tech, Socorro, 167 pp.

Liu, B., Phillips, F.M., Fabryka-Martin, J.T., Fowler, M.M., Stone, W.D., 1994. Cosmogenic ^{36}Cl accumulation in unstable landforms: 1. Effects of the thermal neutron distribution. Water Resour. Res. 30, 3115–3125, (31, 1159).

Phillips, F.M., Zreda, M.G., Flinsch, M.R., Elmore, D., Sharma, P., 1996. A reevaluation of cosmogenic ^{36}Cl production rates in terrestrial rocks. Geophys. Res. Lett. 23, 949–952.

Stone, J., Evans, J., Fifield, K., Cresswell, R., Allan, G., 1996. Cosmogenic chlorine-36 production rates from calcium and potassium. Radiocarbon 38, 172.

Stone, J.O.H., Evans, J.M., Fifield, L.K., Allan, G.L., Cresswell, R.G., 1998. Cosmogenic chlorine-36 production in calcite by muons. Geochim. Cosmochim. Acta 62, 433–454.

Swanson, T., 1996. Determination of ^{36}Cl production rates from the deglaciation history of Whidbey and Fidalgo Islands, Washington (abstr.). Radiocarbon 38 (1), 172.

Yamashita, M., Stephens, L.D., Patterson, H.W., 1966. Cosmic-ray-produced neutrons at ground level: neutron production rate and flux distribution. J. Geophys. Res. 71, 3817–3834.

Zreda, M.G., Phillips, F.M., Kubik, P.W., Sharma, P., Elmore, D., 1993. Cosmogenic ^{36}Cl dating of a young basaltic eruption complex, Lathrop Wells, Nevada. Geology 21, 57–60.